Deliverable report

D4.3 – Generation of experimental data for modelling (CO conversion)

WP4 – Validation of product valorization

Project Information	
Grant Agreement n°	101058100
Project Dates	September 1st 2022 – August 31st 2025

Funded by the European Union

Horizon Europe Grant Agreement n°101058100
e-CODUCT RESTRICTED – Under Consortium Agreement

Funded by the European Union

Document status

DOCUMENT INFORMATION

Project Name	e-CODUCT
Deliverable Title/Number	D4.3
Deliverable Name	Generation of experimental data for modelling
Responsible beneficiary	UGent
Contributing beneficiaries	#
Contractual delivery date:	31/08/25
Actual delivery date:	31/08/25
Dissemination level	PU

DOCUMENT APPROVAL

Name	Organisation	Role	Action	Date
Joris Thybaut	UGENT	Project Coordinator	Approval	
Gleb Veryasov	TOTB	Technical Coordinator	Approval	
Philippe Lenain	Benkei	Administrative manager	Approval	

DOCUMENT HISTORY

Version	Date	Modifications	Authors
V0	24/08/2025	Draft	S. Zareghorbaei
V1	25/08/2025	Revision	J.Lauwaert
V2	26/08/2025	Draft	Anze Prasnikar
V3	28/08/2025	Revision	Hilde Poelman

To request a change to this document, contact the Document Author.

CONFIGURATION MANAGEMENT

Nature of Deliverable		
R	Document, report (excluding the periodic and final reports)	X
DEC	Websites, patents filing, press & media actions, videos, etc.	
DEM	Demonstrator, pilot, prototype, plan designs	
OTHER	Software, technical diagram, algorithms, models, etc.	
ETHICS	Deliverables related to ethics issues.	

DATA	Data sets, microdata, etc.	
DMP	DATA MANAGEMENT PLAN	
Dissemination level		
PU	Public, fully open, e.g., web (Deliverables flagged as public will be automatically published in CORDIS projects.)	X
SEN	Sensitive, limited under the conditions of the Grant Agreement	

ACRONYM/ABBREVIATIONS	
CA	Consortium Agreement (contractual document between members of the consortium)
DoA	Description of Action (technical annex to the Grant Agreement)
EC	European Commission
EU	European Union
FTP	Funding and Tenders Portal: https://ec.europa.eu/info/funding-tenders/opportunities/portal/screen/home
GA	Grant Agreement (contractual document between EC and beneficiaries)
IPR	Intellectual Property Rights
KO	Kick Off (meeting)
MC	Management Coordinator
MTA	Milestones Trend Analysis
PC	Project Coordinator
PMO	Project Management Office
TL	Task Leaders
WP	Work Package
WPL	Work Package Leaders

Acknowledgements

The information and views set out in this report are those of the author(s) and do not necessarily reflect the official opinion of the European Union. Neither the European Union institutions and bodies nor any person acting on their behalf may be held responsible for the use which may be made of the information contained therein. Reproduction is authorized, provided the source is acknowledged.

Disclaimer

Funded by the European Union. Views and opinions expressed are those of the author(s) only and do not necessarily reflect those of the European Union. Neither the European Union nor the granting authority can be held responsible for them.

Contents

1 Executive summary 7

1.1 Deliverable content 7

1.2 Brief description of the state-of-the-art 7

1.3 Corrective action (if relevant) 7

1.4 IPR issue (if applicable) 7

2 Deliverable report 8

2.1 Context 8

2.2 Brief description of the state-of-the-art 8

2.3 Results obtained 8

2.3.1 Experimental setup 8

2.3.2 Sample preparation 9

2.3.3 Experimental Conditions 10

2.3.4 Methanol formation results 10

2.4 Data Availability 15

2.5 Impact of the results 15

3 Conclusion 15

4 Reference 16

5 Appendix: Raw data of different experiments 17

5.1 Test 1: Temperature effect at different pressures with CO_2 as pure feed. 17

5.2 Test 2: Temperature effect at different pressures with CO as feed. 19

5.3 Test 3: Temperature effect at different pressures with a $CO+CO_2$ feed mixture. 21

5.4 Test 4: WHSV effect with CO_2 as pure feed. 23

List of Tables

Table 1: Catalyst mass and denomination of reactors. 10
Table 2 Detailed experimental conditions and results for reactor comparison tests 11
Table 3 Detailed experimental conditions and results for temperature effect (part I) 18
Table 4 Detailed experimental conditions and results for temperature effect (part II) 20
Table 5 Detailed experimental conditions and results for temperature effect (part III) 22

List of Figures

Figure 1 The scheme of the in-house built parallel packed bed reactor system 9
Figure 2 Filled reactor tube. 9
Figure 3 Comparison of the performance of three reactors under identical reaction conditions (40 bar, H_2/CO_2 = 3, 240 °C, WHSV = 20,000 SmL·(g·h)$^{-1}$). 10
Figure 4 Effect of temperature on methanol mole fraction at different pressure and CO_2/ CO ratio. Top: pure CO_2, middle CO_2/CO=0.16, bottom: pure CO. 12
Figure 5 Effect of WHSV on methanol formation at P = 40 bar, T = 240 °C, feed composition CO_2 = 0.249, H_2 = 0.749. 14
Figure 6 Catalyst deactivation test over 42 h at T = 240 °C, WHSV = 6000 SmL·(h·g)$^{-1}$, and H_2/CO_2 = 3. 14
Figure 7 Effect of temperature on methanol mole fraction at different pressures using CO_2 and H_2 as feed (corresponding operating condition of each point is listed in the table below). 17
Figure 8 Effect of temperature on methanol mole fraction at different pressures using CO and H_2 as feed (corresponding operating condition of each point is listed in the table below). 19
Figure 9 Effect of temperature on methanol mole fraction at different pressures using CO_2, CO and H_2 as feed (corresponding operating condition of each point is listed in the table below). 21
Figure 10 Effect of WHSV on methanol mole fraction at 240 °C, 40 bar (corresponding operating condition of each point is listed in the table below). 23

1 EXECUTIVE SUMMARY

1.1 Deliverable content

The catalytic conversion of CO and CO_2 into methanol was investigated using a commercial $Cu/ZnO/Al_2O_3$ catalyst. Experimental data were generated to support kinetic modeling, with particular emphasis on the effects of operating conditions on the reaction performance. The study further assessed potential operational windows and estimated catalyst cycle length prior to regeneration.

1.2 Brief description of the state-of-the-art

Methanol synthesis from syngas ($CO/CO_2/H_2$) is a well-established industrial process, typically operating under moderate pressures (50–80 bar) and temperatures (200–300°C). Several commercial technologies exist for methanol production at an industrial scale. The two main challenges in this process are catalyst deactivation and equilibrium limitations.

1.3 Corrective action (if relevant)

N.A

1.4 IPR issue (if applicable)

N.A.

2 DELIVERABLE REPORT

Deliverable D4.3 compiles the raw experimental data collected during the methanol production reaction study. It includes the effects of operating conditions on catalyst performance and provides insights into the long-term catalyst activity. These data will be used to validate the kinetic model applied for reactor simulations within WP5.

2.1 Context

D4.3 compiles a comprehensive dataset for methanol synthesis across different operating conditions, including an assessment of long-term catalyst activity. These data are used to select the most appropriate kinetic model, which will underpin the scaled-up reactor modelling in WP5.

2.2 Brief description of the state-of-the-art

Methanol synthesis from CO or CO_2 hydrogenation is a well-established industrial process, typically catalyzed by $Cu/ZnO/Al_2O_3$ under moderate pressures (50–80 bar) and temperatures (200–300°C). Due to thermodynamic limitations, unreacted gases are commonly recycled to the reactor inlet, to increase the overall efficiency. At the industrial scale, several commercial technologies have been developed to optimize methanol production, including the Lurgi, Haldor Topsøe, Mitsubishi, Casale, Johnson Matthey/Davy, Toyo, and Linde processes [1]. Deactivation of the catalyst, which is mainly due to chemical poisoning and thermal sintering, is one of the main challenges of this process [2,3].

2.3 Results obtained

2.3.1 Experimental setup

Catalytic tests were carried out in a parallel system of five reactors of which three were used (R3, R4 and R5) with online gas analysis by gas chromatography (Agilent 490 Micro GC) equipped with TCDs and CP-Molsieve and PoraPlot U columns. A premixed gas ($H_2/CO_2/N_2$ = 61/29/10; TPJ d.o.o., Jesenice), high-purity H_2 (99.999%; Messer) and CO (99.997%) were blended to prepare the reactor feed compositions. The setup scheme is shown in Figure 1.

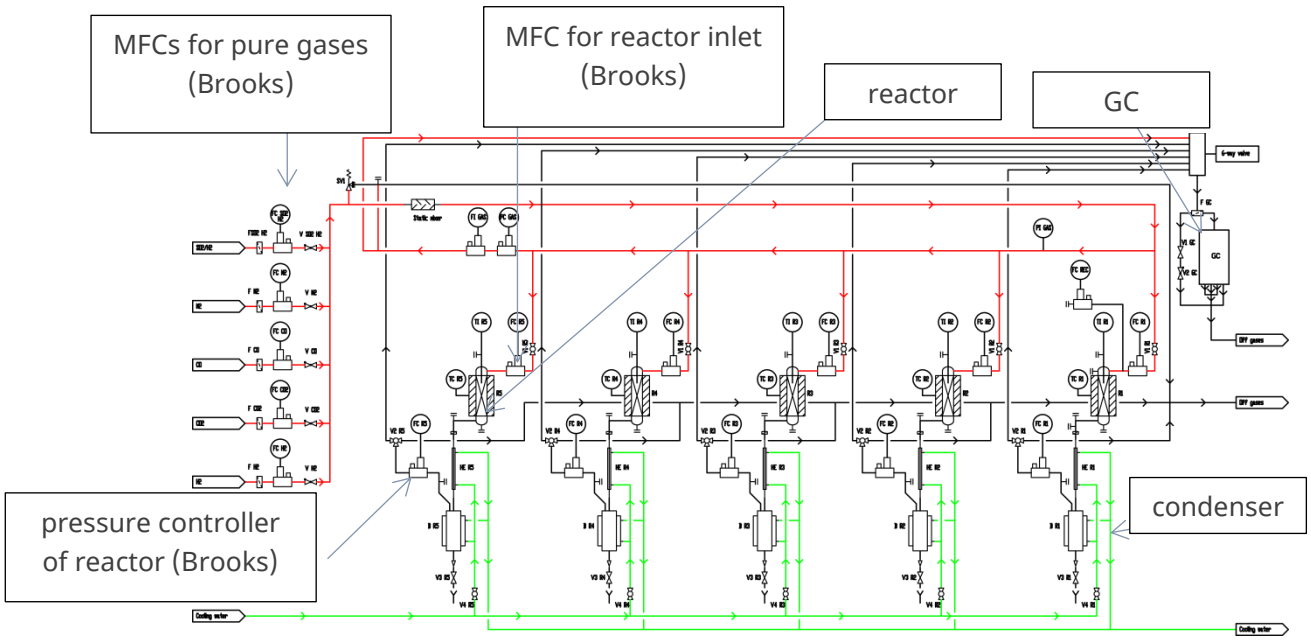

Figure 1 The scheme of the in-house built parallel packed bed reactor system

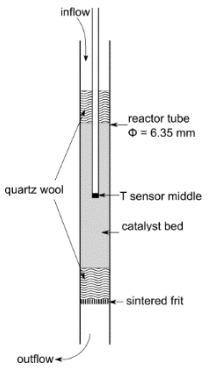

Figure 2 Filled reactor tube.

2.3.2 Sample preparation

Cu/ZnO/Al2O3 methanol synthesis catalyst pellets by Riogen were ground and sieved to obtain a particle size fraction between 150-250 µm. The catalyst was not dried before the catalyst testing, however the dry matter before reaction was determined to be 97.4% (based on drying at 110 °C for 1h). Approximately 0.25 g of pellets were mixed with 1.6 g of SiC (bed length 30 mm) and inserted into a reactor cartridge with an internal diameter (ID) of 6.35 mm.

The catalyst was reduced at 1 bar under a flow of 3% H_2 in N_2 by heating at a rate of 2.5 °C·min^{-1} to 250 °C. The temperature was maintained for 20 min, after which the H_2 concentration was increased stepwise: first to 10% H_2 for 20 min, and then to 100% H_2 for 140 min. The total flow rate in each reactor was 30 SmL·min^{-1}, corresponding to a weight hourly space velocity (WHSV) of 7200 SmL·(g·h)$^{-1}$.

Table 1: Catalyst mass and denomination of reactors.

Reactor	R3	R4	R5
Sample name	R3_Riogen	R4_Riogen	R5_Riogen
Cat. Mass [g]	0.2504	0.251	0.2501
SiC [g]	1.60	1.60	1.60

2.3.3 Experimental Conditions

Following activation, we started with 42 h stabilization test at high conversion (WHSV 6000 SmL/(h g)) to decrease the activity change during condition screening. At several time points we also tested the reactors at standard conditions (40 bar, 20000 SmL/(h g), 240 °C, H_2:CO_2:CO=3:1:0) to check the catalyst state. Catalytic tests were then performed under varying operating conditions in 3 different reactors (R3, R4, R5). The pressure was adjusted between 40 and 80 bar, the $H_2/(CO_2+CO)$ feed ratio was maintained at 2 to 3, the reaction temperature was varied from 200 to 280 °C, and the WHSV was adjusted between 6000 and 20,000 SmL·(g·h)$^{-1}$. The plan was to screen conditions at stoichiometric gas inlet composition under e-CODUCT relevant conditions (among others CO_2 free gas or with small addition of CO_2 at relevant pressures and temperatures).
All reported data points represent the average of two GC measurements. Under steady-state conditions, the relative deviation was consistently below 0.5% (absolute difference of 0.005%) for methanol concentrations above 1% in the gas phase.

2.3.4 Methanol formation results

First of all, the performance of the three reactors was evaluated, and the results presented in Figure 3 and Table 2 indicate no significant initial differences in catalytic behavior among the reactors.

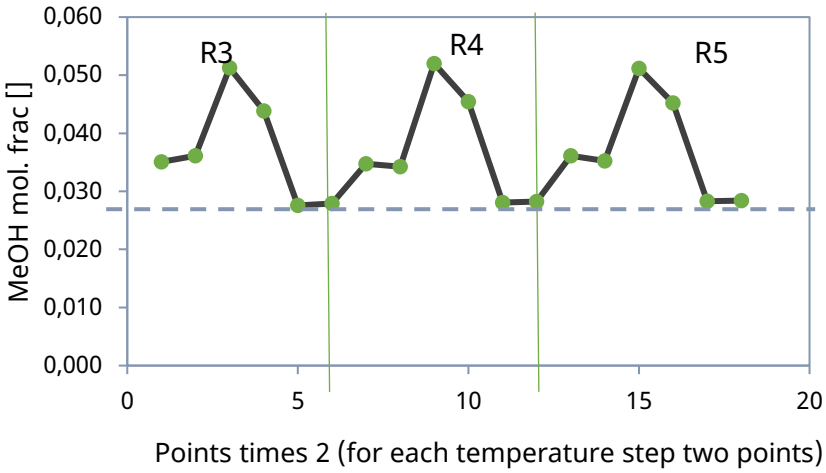

Figure 3 Comparison of the performance of three reactors under identical reaction conditions (40 bar, H_2/CO_2 = 3, 240 °C, WHSV = 20,000 SmL·(g·h)$^{-1}$).

Table 2 Detailed experimental conditions and results for reactor comparison tests

					Inlet- mole fraction			Outlet- mole fraction					
Point	Reactor	T [°C]	WHSV [SmL/(h g)]	p [bara]	H2	CO2	SUM	H2	CO	CO2	H2O	CH3OH	SUM
1	R3	240	20000	40	0.752	0.246	0.998	0.710	0.024	0.198	0.057	0.035	1.024
1	R3	240	20000	40	0.752	0.246	0.998	0.709	0.024	0.198	0.057	0.036	1.025
2	R3	240	6000	40	0.752	0.246	0.998	0.702	0.021	0.193	0.066	0.051	1.033
2	R3	240	6000	40	0.752	0.246	0.998	0.708	0.023	0.192	0.061	0.044	1.029
3	R3	240	20000	40	0.752	0.246	0.998	0.695	0.024	0.223	0.048	0.028	1.018
3	R3	240	20000	40	0.752	0.246	0.998	0.715	0.024	0.204	0.048	0.028	1.020
4	R4	240	20000	40	0.752	0.246	0.998	0.707	0.024	0.200	0.057	0.035	1.024
4	R4	240	20000	40	0.752	0.246	0.998	0.711	0.024	0.198	0.056	0.034	1.023
5	R4	240	6000	40	0.752	0.246	0.998	0.705	0.021	0.189	0.066	0.052	1.034
5	R4	240	6000	40	0.752	0.246	0.998	0.708	0.023	0.191	0.063	0.045	1.030
6	R4	240	20000	40	0.752	0.246	0.998	0.711	0.024	0.207	0.049	0.028	1.019
6	R4	240	20000	40	0.752	0.246	0.998	0.714	0.024	0.204	0.049	0.028	1.020
7	R5	240	20000	40	0.752	0.246	0.998	0.709	0.025	0.198	0.057	0.036	1.025
7	R5	240	20000	40	0.752	0.246	0.998	0.713	0.025	0.195	0.056	0.035	1.024
8	R5	240	6000	40	0.752	0.246	0.998	0.706	0.021	0.189	0.066	0.051	1.033
8	R5	240	6000	40	0.752	0.246	0.998	0.707	0.023	0.191	0.063	0.045	1.029
9	R5	240	20000	40	0.752	0.246	0.998	0.713	0.025	0.204	0.050	0.028	1.020
9	R5	240	20000	40	0.752	0.246	0.998	0.714	0.025	0.203	0.050	0.028	1.020

To investigate the effect of the key operating conditions (temperature, pressure, WHSV, and feed composition) on the methanol synthesis performance, four different experiments were conducted. The corresponding raw data, which are discussed later in this section, are provided in the Appendix and can be referred to using the following codes:

- **Test 1:** Effect of temperature at varying pressures using CO_2 as pure feed.
- **Test 2:** Effect of temperature at varying pressures using CO as feed.
- **Test 3:** Effect of temperature at varying pressures using a $CO+CO_2$ feed mixture.
- **Test 4:** Effect of WHSV using CO_2 as pure feed.

Figure 4 illustrates the impact of temperature across different pressures and feed compositions. In the case of pure CO_2 as feed (top plot), the methanol mole fraction increases with temperature up to around 260 °C, after which it declines, indicating the equilibrium limitation of the reaction. A clear pressure dependence is observed: higher pressures lead to increased methanol formation.

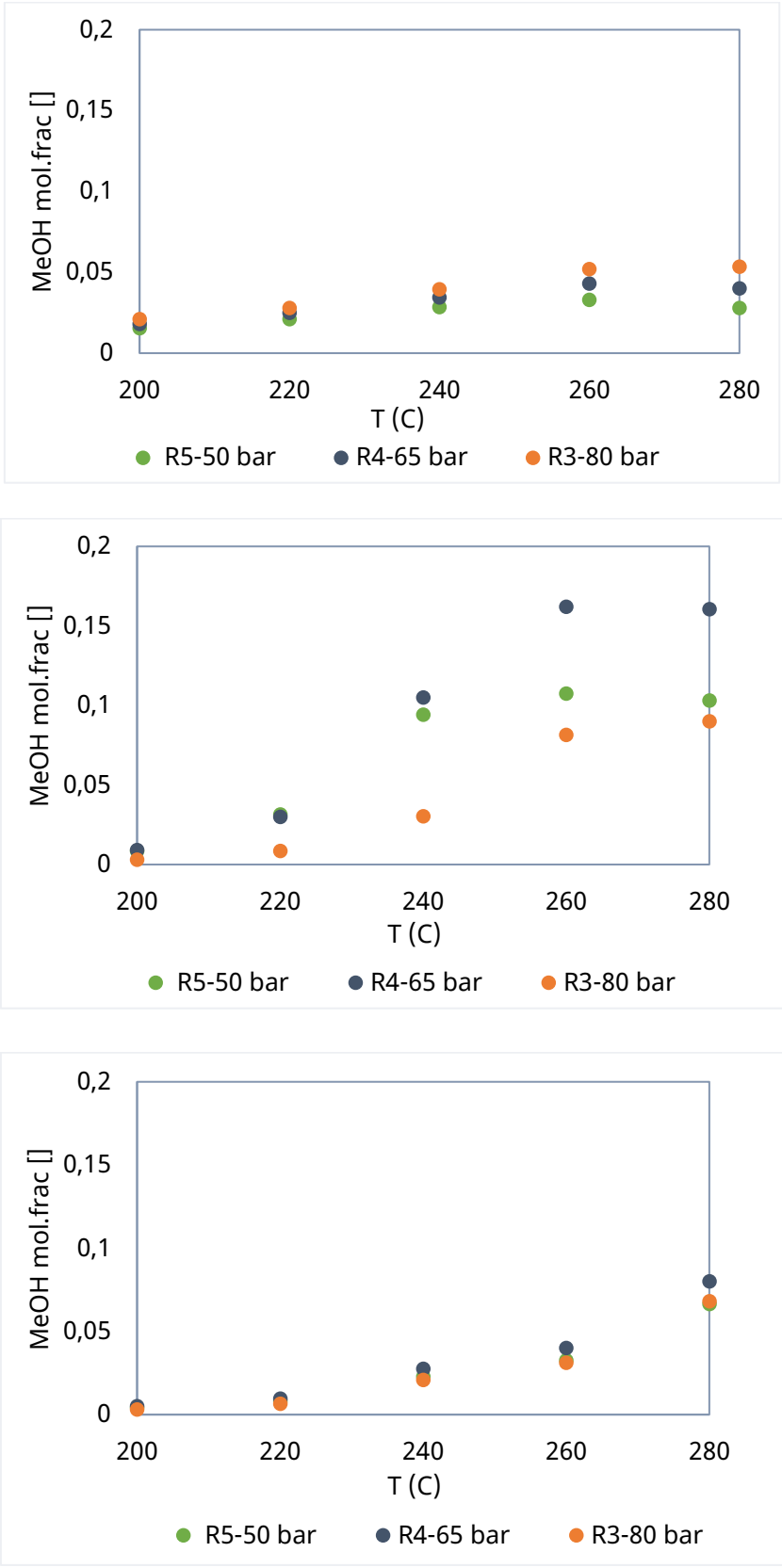

Figure 4 Effect of temperature on methanol mole fraction at different pressure and CO_2/ CO ratio. Top: pure CO_2, middle CO_2/CO=0.16, bottom: pure CO.

For the case of a CO–CO_2 mixture as feed (middle plot), the methanol production is the highest when compared to the pure CO and pure CO_2 feeds, with the reaction being thermodynamically limited at around 280 °C. Unlike the pure CO_2 case, the pressure effect here is less straightforward: methanol formation does not increase monotonically with pressure, and the amount obtained at 80 bar is lower than that observed at 50 and 65 bar.

Finally, for the case of pure CO as feed (bottom plot), the behavior of methanol formation at 80 bar is similar to that obtained with the CO-CO_2 mixture and remains lower than the values observed at 50 and 65 bar. However, the overall pressure dependency is less pronounced than in the other two cases. Under these conditions, the methanol mole fraction increases steadily with temperature at each pressure, and no clear effect of thermodynamic limitation is observed up to 280 °C. It is important to note the effect of deactivation. We first conducted the test with a CO-free mixture, then with a CO_2-free mixture and eventually with the CO_2-CO-H_2 mixture. When the catalyst was exposed to a CO_2-free mixture the catalyst activity dropped especially in the case of R3 at the highest pressure (80 bar). The final outlet MeOH molar fractions at standard condition at the end of screening were 2.2%, 2.6% and 2.7% for R3, R4 and R5, respectively (starting at 2.8% after the stabilization step). Therefore, the reversed trend at increasing pressure from 65 bar to 80 bar could be due to deactivation.

To further explain this difference, in the case of CO_2-free gas, we observe some H_2O and CO_2. It is suspected that irreversible deactivation is caused by carbon deposition through Boudouard reaction. At elevated temperature and pressure this reaction is more pronounced, which is supported by GC measurements and deactivation trends.

The different behaviors observed at varying temperatures, pressures, and feed compositions can be explained by the underlying reaction pathways involved in methanol formation. These include CO hydrogenation, the reverse water–gas shift reaction, and CO_2 hydrogenation, as outlined below:

$$CO + 2H_2 \leftrightarrow CH_3OH \qquad \Delta H = -90.5\frac{kJ}{mol} \qquad (I)$$

$$CO_2 + H_2 \leftrightarrow CO + H_2O \qquad \Delta H = +41\frac{kJ}{mol} \qquad (II)$$

$$CO_2 + 3H_2 \leftrightarrow CH_3OH + H_2O \qquad \Delta H = -49.5\frac{kJ}{mol} \qquad (III)$$

Depending on the operating conditions, the dominant reaction pathway, whether determined by kinetic or thermodynamic factors, varies, and this directly impacts the observed behavior of methanol formation.

The effect of WHSV on methanol formation was investigated by conducting three tests at different WHSV values (6,000; 20,000; and 33,000 SmL/(h·g)) under identical conditions of 240 °C, 40 bar, and CO_2 as the only carbon source (see Figure 5). As shown in this figure, increasing the space velocity reduces the residence time in the reactor, which in turn decreases the amount of methanol detected at the outlet.

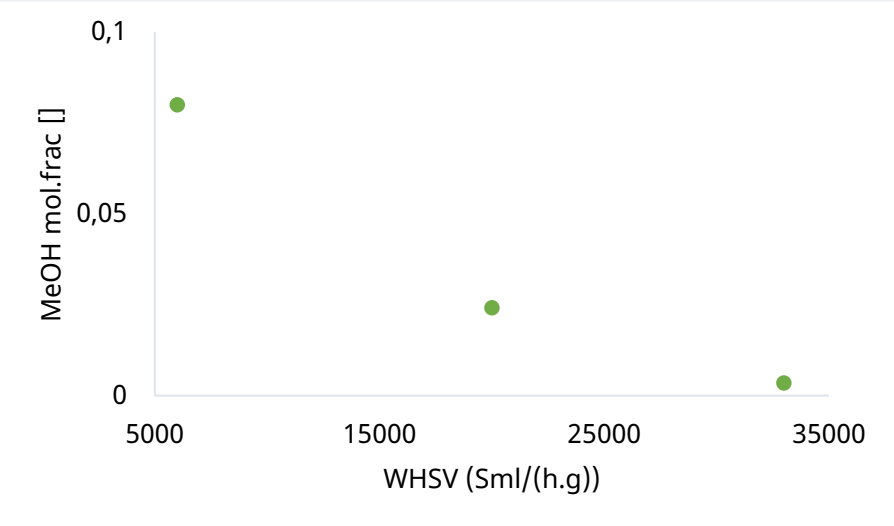

Figure 5 Effect of WHSV on methanol formation at P = 40 bar, T = 240 °C, feed composition CO_2 = 0.249, H_2 = 0.749.

To investigate catalyst deactivation over extended time-on-stream, an experiment was conducted under high-conversion conditions (40 bar, H_2/CO_2 = 3, 240 °C, WHSV = 6000 SmL·(g·h)$^{-1}$) for a duration of 42 h in all three reactors (R3, R4, and R5), as shown in Figure 6. According to the results in Figure 6, after 42 h on stream the methanol mole fraction decreased from 0.051 to about 0.045, corresponding to an 11.7% decline.

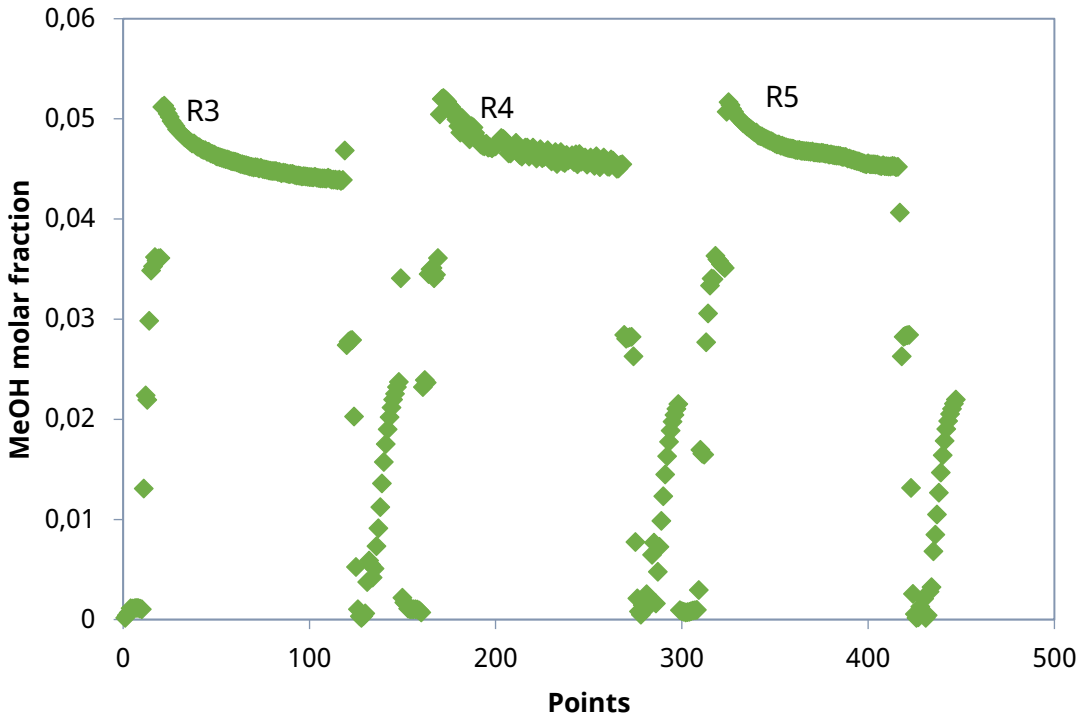

Figure 6 Catalyst deactivation test over 42 h at T = 240 °C, WHSV = 6000 SmL·(h·g)$^{-1}$, and H_2/CO_2 = 3.

2.4 Data Availability

The deliverable report is public, while further data is available upon request.

2.5 Impact of the results

The experimental data obtained in this study provide a solid basis for selecting and validating the most appropriate kinetic model. Such a model can then be applied to predict the behavior of non-ideal industrial reactors operating with this catalyst, as part of WP5. In addition, the data offer valuable insights into the influence of different operating conditions on reaction performance and methanol formation. Ultimately, this knowledge enables the identification and optimization of the most suitable operating window for the methanol synthesis reaction.

3 CONCLUSION

In this work, the performance of a commercial $Cu/ZnO/Al_2O_3$ methanol synthesis catalyst was systematically investigated under a wide range of operating conditions. The effects of temperature, pressure, feed composition, and WHSV on methanol formation were examined through different experiments, while catalyst stability was assessed in a 42 h time-on-stream experiment.

The results demonstrate that using CO_2 as the sole carbon source in the feed leads to lower methanol yields compared to when pure CO is used, whereas a mixture of CO and CO_2 in the feed leads to an increased methanol mole fraction. The results revealed clear dependencies of methanol production on operating conditions, with one of the three principal reaction pathways, CO hydrogenation, CO_2 hydrogenation, or the reverse water–gas shift, becoming dominant depending on the regime.

The effect of WHSV highlighted the role of residence time, with lower space velocities favoring higher methanol yields. Catalyst deactivation was moderate, with an 11.7% decrease in methanol mole fraction observed over 42 h under high-conversion conditions. Overall, the generated dataset provides a reliable basis for kinetic model selection and validation, enabling accurate prediction of catalyst behavior in non-ideal industrial reactors.

4 REFERENCE

[1] M. Ebrahimzadeh Sarvestani, O. Norouzi, F. Di Maria, A. Dutta, From catalyst development to reactor Design: A comprehensive review of methanol synthesis techniques, Energy Convers Manag 302 (2024). https://doi.org/10.1016/j.enconman.2024.118070.

[2] M.R. Rahimpour, J. Fathikalajahi, A. Jahanmiri, Selective kinetic deactivation model for methanol synthesis from simultaneous reaction of CO2 and CO with H2 on a commercial copper/zinc oxide catalyst, Canadian Journal of Chemical Engineering 76 (1998) 753–761. https://doi.org/10.1002/cjce.5450760410.

[3] Ingvild Lovik, Modelling, Estimation and Optimization of the Methanol Synthesis with Catalyst Deactivation., Norwegian University of Science and Technology, 2001.

5 APPENDIX: RAW DATA OF DIFFERENT EXPERIMENTS

5.1 Test 1: Temperature effect at different pressures with CO_2 as pure feed.

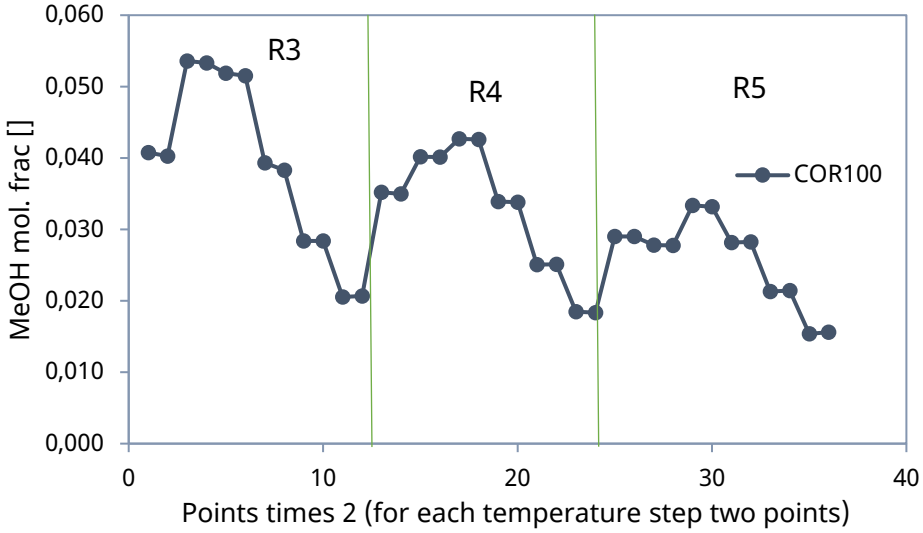

Figure 7 Effect of temperature on methanol mole fraction at different pressures using CO_2 and H_2 as feed (corresponding operating condition of each point is listed in the table below).

Table 3 Detailed experimental conditions and results for temperature effect (part I)

						Inlet composition-mol. frac. [%/100]					Outlet composition-mol. frac. [%/100]						
Point	Reactor	Temperature [°C]	Start/End of condition	WHSV [SmL/(h g)]	p [bara]	Inlet H2	Inlet CO2	Inlet CO	Inlet N2	SUM	H2	O2/N2	CO	CO2	H2O	CH3OH	SUM
1	R3	240	start	2.00E+04	80	0.653	0.254	0.000	0.085	0.992	0.578	0.099	0.022	0.217	0.058	0.041	1.016
1	R3	240	end	2.00E+04	80	0.653	0.254	0.000	0.085	0.992	0.600	0.090	0.022	0.206	0.057	0.040	1.015
2	R3	280	start	2.00E+04	80	0.653	0.254	0.000	0.085	0.992	0.583	0.093	0.029	0.191	0.075	0.054	1.024
2	R3	280	end	2.00E+04	80	0.653	0.254	0.000	0.085	0.992	0.584	0.092	0.027	0.193	0.074	0.053	1.024
3	R3	260	start	2.00E+04	80	0.653	0.254	0.000	0.085	0.992	0.587	0.092	0.025	0.197	0.070	0.052	1.023
3	R3	260	end	2.00E+04	80	0.653	0.254	0.000	0.085	0.992	0.587	0.092	0.025	0.197	0.070	0.052	1.022
4	R3	240	start	2.00E+04	80	0.653	0.254	0.000	0.085	0.992	0.600	0.090	0.022	0.207	0.057	0.039	1.016
4	R3	240	end	2.00E+04	80	0.653	0.254	0.000	0.085	0.992	0.603	0.090	0.022	0.208	0.055	0.038	1.016
5	R3	220	start	2.00E+04	80	0.653	0.254	0.000	0.085	0.992	0.620	0.088	0.011	0.225	0.036	0.028	1.010
5	R3	220	end	2.00E+04	80	0.653	0.254	0.000	0.085	0.992	0.620	0.088	0.011	0.225	0.036	0.028	1.009
6	R3	200	start	2.00E+04	80	0.653	0.254	0.000	0.085	0.992	0.633	0.087	0.004	0.237	0.022	0.021	1.004
6	R3	200	end	2.00E+04	80	0.653	0.254	0.000	0.085	0.992	0.633	0.087	0.004	0.238	0.022	0.021	1.004
7	R4	240	start	2.00E+04	65	0.653	0.254	0.000	0.085	0.992	0.589	0.096	0.022	0.216	0.054	0.035	1.012
7	R4	240	end	2.00E+04	65	0.653	0.254	0.000	0.085	0.992	0.604	0.089	0.022	0.209	0.053	0.035	1.012
8	R4	280	start	2.00E+04	65	0.653	0.254	0.000	0.085	0.992	0.592	0.090	0.033	0.194	0.068	0.040	1.018
8	R4	280	end	2.00E+04	65	0.653	0.254	0.000	0.085	0.992	0.592	0.090	0.033	0.194	0.068	0.040	1.018
9	R4	260	start	2.00E+04	65	0.653	0.254	0.000	0.085	0.992	0.594	0.091	0.027	0.200	0.064	0.043	1.018
9	R4	260	end	2.00E+04	65	0.653	0.254	0.000	0.085	0.992	0.594	0.091	0.027	0.200	0.064	0.043	1.018
10	R4	240	start	2.00E+04	65	0.653	0.254	0.000	0.085	0.992	0.606	0.089	0.022	0.209	0.052	0.034	1.012
10	R4	240	end	2.00E+04	65	0.653	0.254	0.000	0.085	0.992	0.606	0.089	0.022	0.210	0.052	0.034	1.013
11	R4	220	start	2.00E+04	65	0.653	0.254	0.000	0.085	0.992	0.623	0.088	0.011	0.227	0.034	0.025	1.007
11	R4	220	end	2.00E+04	65	0.653	0.254	0.000	0.085	0.992	0.623	0.088	0.011	0.227	0.033	0.025	1.007
12	R4	200	start	2.00E+04	65	0.653	0.254	0.000	0.085	0.992	0.635	0.087	0.004	0.239	0.020	0.018	1.003
12	R4	200	end	2.00E+04	65	0.653	0.254	0.000	0.085	0.992	0.634	0.087	0.003	0.239	0.020	0.018	1.002
13	R5	240	start	2.00E+04	50	0.653	0.254	0.000	0.085	0.992	0.595	0.095	0.024	0.217	0.049	0.029	1.009
13	R5	240	end	2.00E+04	50	0.653	0.254	0.000	0.085	0.992	0.609	0.089	0.024	0.211	0.049	0.029	1.010
14	R5	280	start	2.00E+04	50	0.653	0.254	0.000	0.085	0.992	0.599	0.088	0.038	0.196	0.061	0.028	1.011
14	R5	280	end	2.00E+04	50	0.653	0.254	0.000	0.085	0.992	0.600	0.088	0.038	0.197	0.061	0.028	1.012
15	R5	260	start	2.00E+04	50	0.653	0.254	0.000	0.085	0.992	0.600	0.089	0.031	0.202	0.059	0.033	1.014
15	R5	260	end	2.00E+04	50	0.653	0.254	0.000	0.085	0.992	0.600	0.089	0.030	0.202	0.059	0.033	1.013
16	R5	240	start	2.00E+04	50	0.653	0.254	0.000	0.085	0.992	0.609	0.088	0.024	0.211	0.048	0.028	1.009
16	R5	240	end	2.00E+04	50	0.653	0.254	0.000	0.085	0.992	0.610	0.088	0.025	0.211	0.048	0.028	1.011
17	R5	220	start	2.00E+04	50	0.653	0.254	0.000	0.085	0.992	0.626	0.087	0.011	0.230	0.030	0.021	1.006
17	R5	220	end	2.00E+04	50	0.653	0.254	0.000	0.085	0.992	0.626	0.087	0.011	0.229	0.030	0.021	1.006
18	R5	200	start	2.00E+04	50	0.653	0.254	0.000	0.085	0.992	0.637	0.086	0.004	0.241	0.018	0.015	1.002
18	R5	200	start	2.00E+04	50	0.653	0.254	0.000	0.085	0.992	0.637	0.086	0.003	0.241	0.018	0.016	1.001

5.2 Test 2: Temperature effect at different pressures with CO as feed.

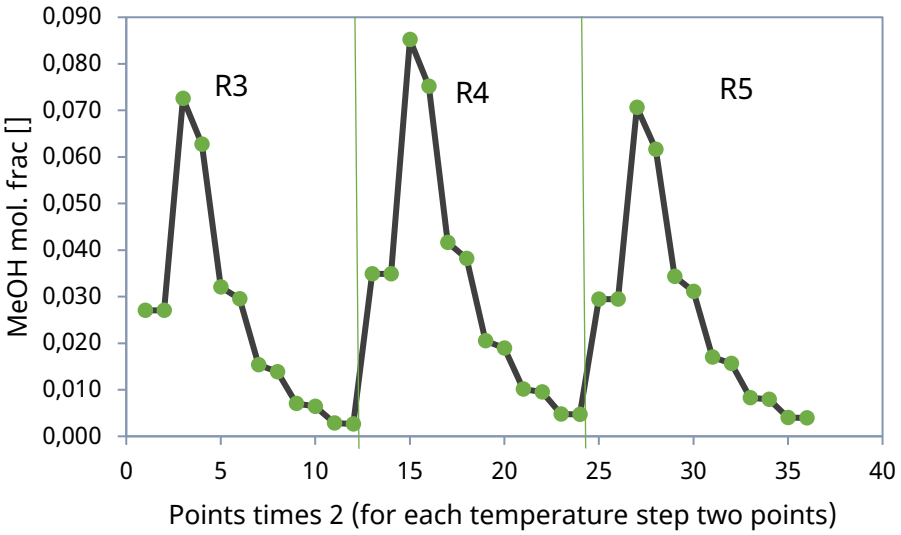

Figure 8 Effect of temperature on methanol mole fraction at different pressures using CO and H_2 as feed (corresponding operating condition of each point is listed in the table below).

Table 4 Detailed experimental conditions and results for temperature effect (part II)

						Inlet composition-mol. frac. [%/100]					Outlet composition-mol. frac. [%/100]						
Point	Reactor	Temperature [°C]	Start/End of condition	WHSV [SmL/(h g)]	p [bara]	Inlet H2	Inlet CO2	Inlet CO	Inlet N2	SUM	H2	O2/N2	CO	CO2	H2O	CH3OH	SUM
1	R3	240	start	2.00E+04	80	0.650	0.000	0.333	0.000	0.982	0.642	0.000	0.320	0.002	0.002	0.027	0.993
1	R3	240	end	2.00E+04	80	0.650	0.000	0.333	0.000	0.982	0.642	0.000	0.320	0.002	0.002	0.027	0.993
2	R3	280	start	2.00E+04	80	0.650	0.000	0.333	0.000	0.982	0.629	0.000	0.305	0.003	0.002	0.073	1.012
2	R3	280	end	2.00E+04	80	0.650	0.000	0.333	0.000	0.982	0.632	0.000	0.309	0.002	0.002	0.063	1.008
3	R3	260	start	2.00E+04	80	0.650	0.000	0.333	0.000	0.982	0.642	0.000	0.321	0.001	0.002	0.032	0.998
3	R3	260	end	2.00E+04	80	0.650	0.000	0.333	0.000	0.982	0.643	0.000	0.322	0.001	0.002	0.030	0.997
4	R3	240	start	2.00E+04	80	0.650	0.000	0.333	0.000	0.982	0.647	0.000	0.326	0.001	0.002	0.015	0.991
4	R3	240	end	2.00E+04	80	0.650	0.000	0.333	0.000	0.982	0.648	0.000	0.326	0.000	0.002	0.014	0.990
5	R3	220	start	2.00E+04	80	0.650	0.000	0.333	0.000	0.982	0.649	0.000	0.329	0.000	0.001	0.007	0.987
5	R3	220	end	2.00E+04	80	0.650	0.000	0.333	0.000	0.982	0.650	0.000	0.329	0.000	0.001	0.006	0.987
6	R3	200	start	2.00E+04	80	0.650	0.000	0.333	0.000	0.982	0.651	0.000	0.330	0.000	0.001	0.003	0.985
6	R3	200	end	2.00E+04	80	0.650	0.000	0.333	0.000	0.982	0.651	0.000	0.331	0.000	0.001	0.003	0.986
7	R4	240	start	2.00E+04	65	0.650	0.000	0.333	0.000	0.982	0.640	0.000	0.318	0.002	0.002	0.035	0.997
7	R4	240	end	2.00E+04	65	0.650	0.000	0.333	0.000	0.982	0.640	0.000	0.318	0.002	0.002	0.035	0.997
8	R4	280	start	2.00E+04	65	0.650	0.000	0.333	0.000	0.982	0.626	0.000	0.300	0.004	0.002	0.085	1.017
8	R4	280	end	2.00E+04	65	0.650	0.000	0.333	0.000	0.982	0.629	0.000	0.303	0.003	0.002	0.075	1.012
9	R4	260	start	2.00E+04	65	0.650	0.000	0.333	0.000	0.982	0.638	0.000	0.316	0.001	0.002	0.042	0.999
9	R4	260	end	2.00E+04	65	0.650	0.000	0.333	0.000	0.982	0.640	0.000	0.318	0.001	0.002	0.038	0.999
10	R4	240	start	2.00E+04	65	0.650	0.000	0.333	0.000	0.982	0.645	0.000	0.324	0.000	0.002	0.021	0.992
10	R4	240	end	2.00E+04	65	0.650	0.000	0.333	0.000	0.982	0.646	0.000	0.324	0.000	0.002	0.019	0.991
11	R4	220	start	2.00E+04	65	0.650	0.000	0.333	0.000	0.982	0.648	0.000	0.328	0.000	0.001	0.010	0.988
11	R4	220	end	2.00E+04	65	0.650	0.000	0.333	0.000	0.982	0.649	0.000	0.329	0.000	0.001	0.009	0.989
12	R4	200	start	2.00E+04	65	0.650	0.000	0.333	0.000	0.982	0.650	0.000	0.331	0.000	0.001	0.005	0.987
12	R4	200	end	2.00E+04	65	0.650	0.000	0.333	0.000	0.982	0.650	0.000	0.330	0.000	0.001	0.005	0.986
13	R5	240	start	2.00E+04	50	0.650	0.000	0.333	0.000	0.982	0.641	0.000	0.321	0.001	0.002	0.029	0.995
13	R5	240	end	2.00E+04	50	0.650	0.000	0.333	0.000	0.982	0.641	0.000	0.321	0.001	0.002	0.029	0.995
14	R5	280	start	2.00E+04	50	0.650	0.000	0.333	0.000	0.982	0.630	0.000	0.303	0.004	0.002	0.071	1.010
14	R5	280	end	2.00E+04	50	0.650	0.000	0.333	0.000	0.982	0.632	0.000	0.308	0.003	0.002	0.062	1.007
15	R5	260	start	2.00E+04	50	0.650	0.000	0.333	0.000	0.982	0.640	0.000	0.320	0.001	0.002	0.034	0.997
15	R5	260	end	2.00E+04	50	0.650	0.000	0.333	0.000	0.982	0.642	0.000	0.321	0.001	0.002	0.031	0.996
16	R5	240	start	2.00E+04	50	0.650	0.000	0.333	0.000	0.982	0.646	0.000	0.326	0.000	0.001	0.017	0.991
16	R5	240	end	2.00E+04	50	0.650	0.000	0.333	0.000	0.982	0.646	0.000	0.326	0.000	0.001	0.016	0.990
17	R5	220	start	2.00E+04	50	0.650	0.000	0.333	0.000	0.982	0.648	0.000	0.329	0.000	0.001	0.008	0.987
17	R5	220	end	2.00E+04	50	0.650	0.000	0.333	0.000	0.982	0.648	0.000	0.329	0.000	0.001	0.008	0.987
18	R5	200	start	2.00E+04	50	0.650	0.000	0.333	0.000	0.982	0.649	0.000	0.331	0.000	0.001	0.004	0.985
18	R5	200	start	2.00E+04	50	0.650	0.000	0.333	0.000	0.982	0.650	0.000	0.331	0.000	0.001	0.004	0.986

5.3 Test 3: Temperature effect at different pressures with a $CO+CO_2$ feed mixture.

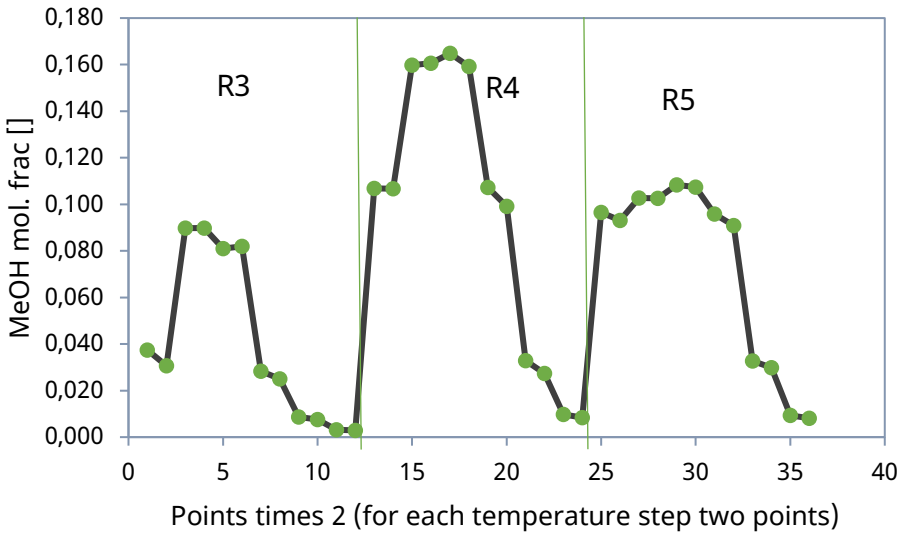

Figure 9 Effect of temperature on methanol mole fraction at different pressures using CO_2, CO and H_2 as feed (corresponding operating condition of each point is listed in the table below).

Table 5 Detailed experimental conditions and results for temperature effect (part III)

						Inlet composition-mol. frac. [%/100]					Outlet composition-mol. frac. [%/100]						
Point	Reactor	Temperature [°C]	Start/End of condition	WHSV [SmL/(hg)]	p [bara]	Inlet H2	Inlet CO2	Inlet CO	Inlet N2	SUM	H2	O2/N2	CO	CO2	H2O	CH3OH	SUM
1	R3	240	start	2.00E+04	80	0.646	0.046	0.277	0.015	0.985	0.635	0.018	0.263	0.042	0.005	0.037	1.001
1	R3	240	end	2.00E+04	80	0.646	0.046	0.277	0.015	0.985	0.636	0.017	0.267	0.042	0.005	0.031	0.998
2	R3	280	start	2.00E+04	80	0.646	0.046	0.277	0.015	0.985	0.616	0.021	0.233	0.055	0.004	0.090	1.020
2	R3	280	end	2.00E+04	80	0.646	0.046	0.277	0.015	0.985	0.617	0.021	0.233	0.055	0.004	0.090	1.020
3	R3	260	start	2.00E+04	80	0.646	0.046	0.277	0.015	0.985	0.619	0.018	0.246	0.047	0.006	0.081	1.017
3	R3	260	end	2.00E+04	80	0.646	0.046	0.277	0.015	0.985	0.620	0.018	0.245	0.047	0.006	0.082	1.018
4	R3	240	start	2.00E+04	80	0.646	0.046	0.277	0.015	0.985	0.636	0.016	0.269	0.042	0.006	0.028	0.997
4	R3	240	end	2.00E+04	80	0.646	0.046	0.277	0.015	0.985	0.637	0.016	0.270	0.042	0.005	0.025	0.996
5	R3	220	start	2.00E+04	80	0.646	0.046	0.277	0.015	0.985	0.643	0.016	0.276	0.042	0.004	0.009	0.989
5	R3	220	end	2.00E+04	80	0.646	0.046	0.277	0.015	0.985	0.644	0.016	0.275	0.042	0.004	0.008	0.988
6	R3	200	start	2.00E+04	80	0.646	0.046	0.277	0.015	0.985	0.646	0.016	0.276	0.043	0.003	0.003	0.987
6	R3	200	end	2.00E+04	80	0.646	0.046	0.277	0.015	0.985	0.646	0.016	0.276	0.043	0.003	0.003	0.986
7	R4	240	start	2.00E+04	65	0.646	0.046	0.277	0.015	0.985	0.614	0.020	0.233	0.049	0.005	0.107	1.028
7	R4	240	end	2.00E+04	65	0.646	0.046	0.277	0.015	0.985	0.614	0.019	0.235	0.049	0.005	0.107	1.029
8	R4	280	start	2.00E+04	65	0.646	0.046	0.277	0.015	0.985	0.602	0.022	0.200	0.059	0.005	0.160	1.048
8	R4	280	end	2.00E+04	65	0.646	0.046	0.277	0.015	0.985	0.602	0.021	0.200	0.059	0.005	0.161	1.048
9	R4	260	start	2.00E+04	65	0.646	0.046	0.277	0.015	0.985	0.601	0.022	0.198	0.058	0.005	0.165	1.049
9	R4	260	end	2.00E+04	65	0.646	0.046	0.277	0.015	0.985	0.603	0.021	0.204	0.057	0.005	0.159	1.048
10	R4	240	start	2.00E+04	65	0.646	0.046	0.277	0.015	0.985	0.613	0.018	0.236	0.049	0.005	0.107	1.030
10	R4	240	end	2.00E+04	65	0.646	0.046	0.277	0.015	0.985	0.616	0.018	0.238	0.049	0.005	0.099	1.024
11	R4	220	start	2.00E+04	65	0.646	0.046	0.277	0.015	0.985	0.635	0.016	0.267	0.043	0.005	0.033	1.000
11	R4	220	end	2.00E+04	65	0.646	0.046	0.277	0.015	0.985	0.637	0.016	0.268	0.043	0.005	0.027	0.997
12	R4	200	start	2.00E+04	65	0.646	0.046	0.277	0.015	0.985	0.643	0.016	0.275	0.042	0.004	0.010	0.989
12	R4	200	end	2.00E+04	65	0.646	0.046	0.277	0.015	0.985	0.644	0.016	0.275	0.042	0.004	0.008	0.989
13	R5	240	start	2.00E+04	50	0.646	0.046	0.277	0.015	0.985	0.618	0.019	0.237	0.048	0.004	0.097	1.024
13	R5	240	end	2.00E+04	50	0.646	0.046	0.277	0.015	0.985	0.618	0.019	0.240	0.049	0.004	0.093	1.022
14	R5	280	start	2.00E+04	50	0.646	0.046	0.277	0.015	0.985	0.610	0.021	0.229	0.058	0.004	0.103	1.025
14	R5	280	end	2.00E+04	50	0.646	0.046	0.277	0.015	0.985	0.610	0.021	0.230	0.058	0.004	0.103	1.025
15	R5	260	start	2.00E+04	50	0.646	0.046	0.277	0.015	0.985	0.609	0.021	0.228	0.057	0.004	0.108	1.028
15	R5	260	end	2.00E+04	50	0.646	0.046	0.277	0.015	0.985	0.610	0.021	0.229	0.057	0.004	0.107	1.028
16	R5	240	start	2.00E+04	50	0.646	0.046	0.277	0.015	0.985	0.617	0.018	0.239	0.049	0.004	0.096	1.024
16	R5	240	end	2.00E+04	50	0.646	0.046	0.277	0.015	0.985	0.618	0.018	0.241	0.049	0.004	0.091	1.021
17	R5	220	start	2.00E+04	50	0.646	0.046	0.277	0.015	0.985	0.635	0.016	0.266	0.044	0.004	0.033	0.998
17	R5	220	end	2.00E+04	50	0.646	0.046	0.277	0.015	0.985	0.636	0.016	0.268	0.044	0.004	0.030	0.999
18	R5	200	start	2.00E+04	50	0.646	0.046	0.277	0.015	0.985	0.642	0.016	0.276	0.042	0.004	0.009	0.989
18	R5	200	start	2.00E+04	50	0.646	0.046	0.277	0.015	0.985	0.643	0.016	0.276	0.042	0.004	0.008	0.989

5.4 Test 4: WHSV effect with CO_2 as pure feed.

- Reference test: 40 bar, H_2/CO_2=3, 240 °C, WHSV of 20,000 SmL/(g·h).
- Experiment as given in table

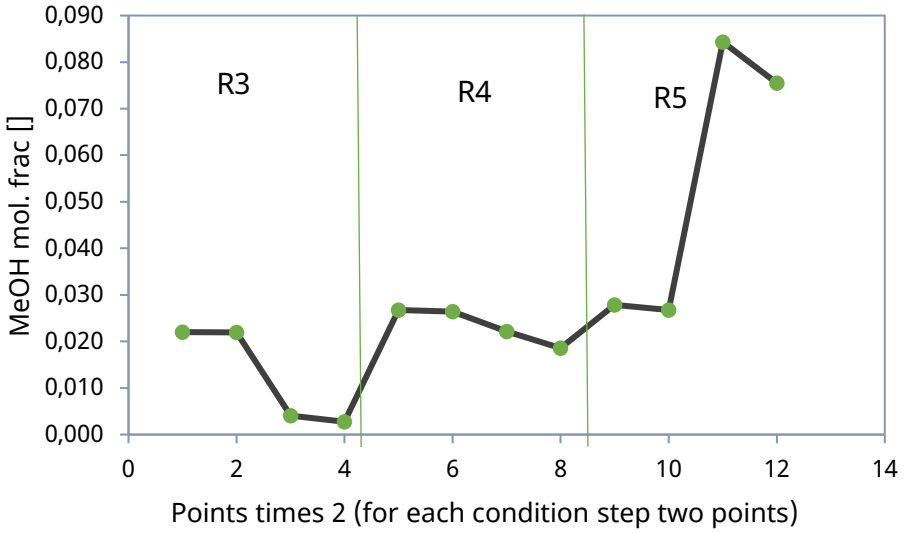

Figure 10 Effect of WHSV on methanol mole fraction at 240 °C, 40 bar (corresponding operating condition of each point is listed in the table below).

						Inlet composition-mol. frac. [%/100]					Outlet composition-mol. frac. [%/100]						
Point	Reactor	Temperature [°C]	Start/End of condition	WHSV [SmL/(h g)]	p [bara]	Inlet H2	Inlet CO2	Inlet CO	Inlet N2	SUM	H2	O2/N2	CO	CO2	H2O	CH3OH	SUM
1	R3	240	start	2.00E+04	40	0.749	0.249	0.000	0.000	0.998	0.724	0.000	0.015	0.220	0.033	0.022	1.014
1	R3	240	end	2.00E+04	40	0.749	0.249	0.000	0.000	0.998	0.725	0.000	0.015	0.218	0.034	0.022	1.014
2	R3	240	start	3.30E+04	40	0.645	0.003	0.337	0.000	0.985	0.643	0.000	0.334	0.005	0.002	0.004	0.987
2	R3	240	end	3.30E+04	40	0.645	0.003	0.337	0.000	0.985	0.653	0.000	0.326	0.004	0.001	0.003	0.987
3	R4	240	start	2.00E+04	40	0.749	0.249	0.000	0.000	0.998	0.719	0.000	0.021	0.208	0.044	0.027	1.018
3	R4	240	end	2.00E+04	40	0.749	0.249	0.000	0.000	0.998	0.719	0.000	0.022	0.208	0.044	0.026	1.018
4	R4	240	start	2.00E+04	40	0.645	0.003	0.337	0.000	0.985	0.637	0.000	0.329	0.004	0.002	0.022	0.994
4	R4	240	end	2.00E+04	40	0.645	0.003	0.337	0.000	0.985	0.640	0.000	0.331	0.002	0.002	0.019	0.993
5	R5	240	start	2.00E+04	40	0.749	0.249	0.000	0.000	0.998	0.716	0.000	0.022	0.207	0.046	0.028	1.019
5	R5	240	end	2.00E+04	40	0.749	0.249	0.000	0.000	0.998	0.717	0.000	0.022	0.206	0.046	0.027	1.018
6	R5	240	start	6.00E+03	40	0.645	0.003	0.337	0.000	0.985	0.621	0.000	0.304	0.007	0.002	0.084	1.018
6	R5	240	end	6.00E+03	40	0.645	0.003	0.337	0.000	0.985	0.624	0.000	0.308	0.005	0.002	0.076	1.015